TOWARDS COLOURED GLAZED THERMAL SOLAR COLLECTORS

J. Boudaden, R. S-C. Ho and P. Oelhafen
Institut für Physik, University of Basel, Klingelbergstrasse 82, CH-4056 Basel, Switzerland
Tel: 41-61-267-37-15, Fax: 41-61-267-37-82, jamila.boudaden@unibas.ch

A. Schüler, C. Roecker and J. - L. Scartezzini
Laboratoire d'Energie Solaire et de Physique du Bâtiment LESO-PB, Ecole Polytechnique Fédérale de Lausanne (EPFL), Bâtiment LE, CH-1015 Lausanne, Switzerland

Abstract – Multilayers of TiO_2 and SiO_2 dielectric coatings deposited by reactive sputtering have been characterized by X-ray photoelectron spectroscopy (XPS), in-stitu real-time laser reflectometry, spectroscopic ellipsometry and spectrophotometry. Measurements have been performed on individual dielectric layers of TiO_2, SiO_2 and multilayers. The experiments show a good agreement between the different techniques. Optical properties can be modelled properly using a Cauchy dispersion model. The optical constants of an individual layer are confirmed by the optical measurements on more complex multilayer structures. Reflectivity of the three-layer films fulfils the requirements for a first step towards coloured glazed thermal solar collectors.

1. INTRODUCTION

Dielectric thin films are widely employed in various optical devices and components like high-reflection mirrors (Bhattacharyya et al 2001), waveguides (Garapon et al, 1996), narrow-band filters (Ouellette et al, 1991), dyes (Gomeza M.M. et al, 2003) and antireflection or high reflection coatings (Selhofer et al, 1999). The performances of these devices are based on interference effects by alternating layers of high and low refractive indexes.

Different optical properties are obtained by depositing multilayers of two or more different materials. Two important requirements must be fulfilled. On one hand, the optical properties of each layer should be uniform. On the other hand, the interface between two layers should be as smooth as possible for a good modelling. Evaporation coating technique underwent rapid development and became a standard method for optical coating (Zhong DishengXu Guangzhong and Liu Wi, 1991). Afterwards, alternative methods such as chemical vapour deposition (C. Martinet et al, 1997), dip coating (H. Köstlin et al, 1997), sol gel method (Que et al, 2000) and reactive sputtering (Hill, 1997) have been extensively studied. The later allows large area coatings and thickness uniformity combined with high rate deposition (Vergöhl et al, 1999).

TiO_2 is one of the most interesting dielectric materials since it is transparent to visible light, has a high refractive index (at $\lambda = 550$ nm $n = 2.54$ for anatase and 2.75 for rutile), a low absorption (Mardare et al, 2002), a good hardness and forms a stable device with SiO_2 in discrete and mixed coatings (Gluck, et al, 1999). SiO_2 is a low-index material and transparent from the UV to the NIR (Tabata et al, 1996). TiO_2/SiO_2 systems have been extensively used to realize a wide variety of optical devices. (Ouellette et al, 1991) reported on a TiO_2–SiO_2 notch filter prepared by ion beam reactive sputtering. (Wong et al, 1998) have reported the possibility of preparation of optical reflection filter using Helicon plasma sputtering. They have prepared multilayers with a wide range of refractive indexes from (n = 1.47 to 2.2) by mixing TiO_2 and SiO_2.

In modern architecture, large glass planes are used as facades in commercial buildings and glazing in a residential home for day lighting. In our case, reflecting multilayers will be used as a cover for solar collectors. For this purpose the reflecting multilayers consisting of oxides materials have to fulfil some requirements. Firstly, large amount of power from solar radiation must be transmitted through the coatings. Moreover, there is a need for zero or near zero absorption materials to avoid energy loss within the coating. Lastly, another critical factor is a narrow reflection in the visible range fixing the colour of the reflected light.

In this work, we report an experimental study for the preparation of optical multilayer coatings based on TiO_2/SiO_2 dielectric films for solar application. A combination of different refractive index and thickness could help to realize a wide range of reflected colours with an acceptable solar transmission.

In the following we will concentrate on three types of samples:

- single layered samples on substrate (TiO_2 // Si-substrate), (SiO_2 // Si-substrate)
- double layered samples on substrate (SiO_2 / TiO_2 // substrate)
- triple layered samples (TiO_2 / SiO_2 / TiO_2 // substrate).

2. EXPERIMENT

2.1 Thin film deposition

The experiments are performed in a vacuum system that consists of two interconnected chambers: sputtering chamber and photoelectron spectroscopy (PES) chamber.

The high vacuum chamber (Fig. 1) used for the dielectric coatings deposition is pumped down to a typical background pressure below 10^{-6} mbar by a turbo pumping system.

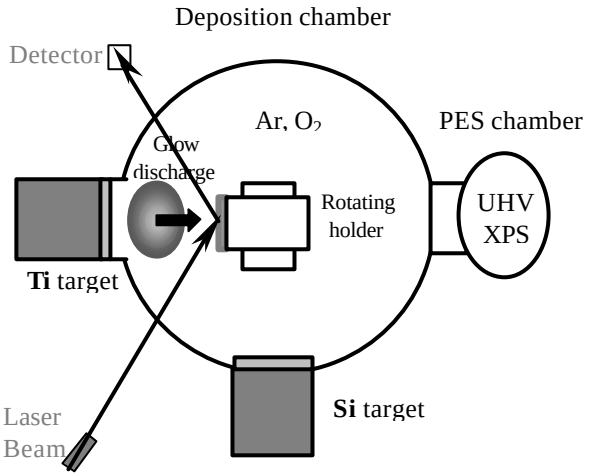

Fig. 1. Experimental setup for dielectric thin film deposition.

The sputtering is carried out in a deposition chamber, using two water-cooled magnetrons capped by titanium and silicon targets. The magnetrons are driven by bipolar-pulsed power (50 - 250 kHz at 250 W) for the Ti target and by medium frequency RF power (100 W at 13.5 kHz) for the Si target. During the thin film deposition carried out at room temperature, the grounded substrate faces the target at a distance between 5 and 8 centimetres. Argon and oxygen are used as process gas and its mass flow ratio is always set to 7:1. A working pressure of around 5 x 10^{-3} mbar is adjusted by throttling the pumping system. Deposition conditions are always run for 4 min before starting a deposition on the chosen substrate in order to achieve stable plasma conditions.

Thin TiO_2 and SiO_2 films are deposited on glass AF45 and monocrystalline silicon (with its native oxide) substrates 4 x 4 cm^2 for the various optical techniques. For the in-situ photoelectron spectroscopy thin films are deposited on sputter cleaned copper substrates.

2.2 Photoelectron spectroscopy

The high vacuum deposition chamber is connected to an ultrahigh vacuum (UHV) electron spectrometer. Samples can be transferred from one system to the other without breaking the vacuum. The electron spectrometer is equipped with a hemispherical analyser (Leybold EA 10/100) and an X-ray source for core level spectroscopy (X-ray photoelectron spectroscopy XPS: Mg $K\alpha$ excitation, $h\upsilon$ = 1253.6 eV). The typical resolution is 0.8 eV for the XPS measurements. A gold sample with the Au $4f_{7/2}$ core level signal at 83.9 eV binding energy is used as a reference for the electron energy calibration.

The relative concentrations of the deposited elements forming the thin films is determined by integration over the Ti 2p, Si 2p and O 1s core level peaks after subtracting a Shirley background (Shirley, 1972). From the photoionization cross-sections given by (Yeh and Lindau, 1985), the atomic concentration at the films surface is calculated using UNIFIT (Hesse, 2002). Charging effects can influence photoelectron spectroscopy measurements of the TiO_2 and SiO_2. In order to avoid the accumulation of positive charge at the sample surface it is necessary to perform the measurements on films not exceeding critical thickness.

2.3 Optical characterization

Silicon substrates have been used for in-situ real-time laser reflectometry and ex-situ ellipsometry while glass substrates have been used for ex-situ spectrophotometry.

The optical reflectivity of a laser beam is measured continuously during the film deposition in order to determine the film thickness, the deposition rate and the optical constants n and k at one wavelength. The analysis of the data is performed using the reflectivity formula of a single layer on the substrate for the numerical fitting (Heavens, 1991). The experimental set up involves an incident laser beam at 532 nm with 1 mW power and a beam diameter of 1 mm (Laser compact, model LCM-T-01 ccs) and the detection of the reflected intensity with a synchronous modulator. The measurement technique is laboratory standard using a chopper, photodiodes, lock-in amplifiers for the sampling of monitor and probe beam (Schüler et al, 2000).

Spectroscopic ellipsometry is a non-destructive optical technique to determine the index of refraction n and the index of extinction k and film thickness of thin layers on a substrate. A monochromatic light beam of known polarization is reflected off the sample at a given angle of incidence altering both the intensity and polarization state of the beam. The method measures the change in the state of polarization of light upon reflection to evaluate the ellipsometry parameters D and Y for each wavelength across the spectral range of interest, thus determining n and k as a function of wavelength. The two parameters are defined as:

$$\tan(\gamma)\exp(iD) = \frac{R_p}{R_s} \qquad (1)$$

where R_p and R_s are the Fresnel reflection coefficients of the sample, with p denoting the direction of the plane of incidence and s the direction perpendicular of the electrical field vector to the incident plane. The optical parameters are then matched to computer models to determine the structure and composition of the sample.

The films on silicon substrates are subjected to ellipsometry measurements, performed by ellipsometer (SENTECH SE 850) in the range of 350 - 800 nm with variable angle of incidence ranging between 40° and 70° by steps of 10° to measure the parameters D and Y.

The total hemispherical reflectance (diffuse and specular) at 7° angle of incidence and transmission at 0° angle of incidence measurements in the UV, VIS and NIR are performed on a Varian Cary 5 spectrophotometer.

3. RESULTS AND DISCUSSION

3.1 XPS

Figure 2 shows the XPS spectra (Ti 2p and O 1s core level) of sputtered titanium dioxide deposited at room temperature.

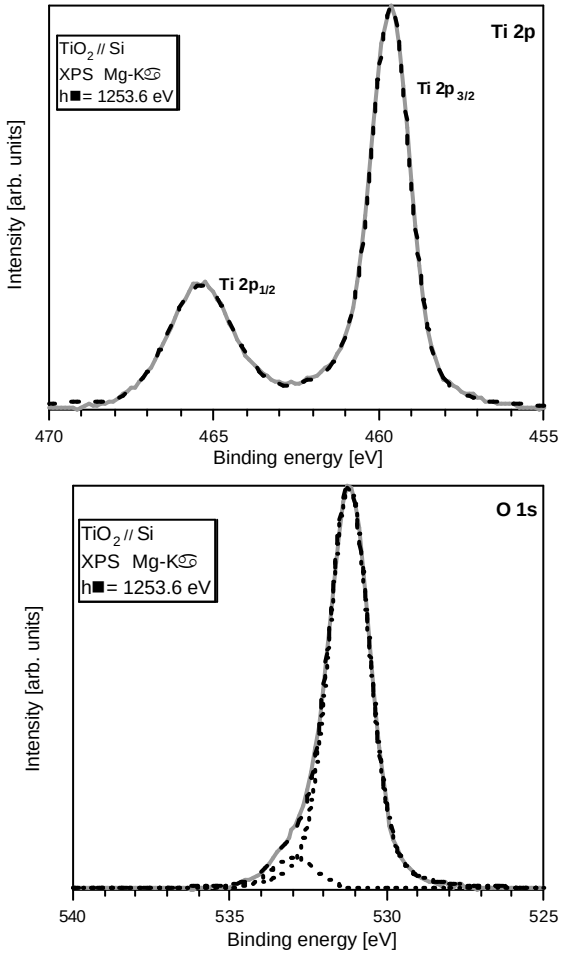

Fig. 2. XPS Ti 2p and O 1s core-level spectra of the TiO_2: the solid line corresponds to the experimental data and the dashed one to the fit peaks

The binding energies of Ti $2p_{3/2}$ and Ti $2p_{1/2}$ are observed at 459.6 eV and 465.4 eV, which correspond to the oxidation state Ti^{4+}. The distance between Ti $2p_{3/2}$ and Ti $2p_{1/2}$ equal to 5.7 eV is in good agreement with bulk TiO_2 (Leprince-Wang, 2002). The ratio of oxygen to titanium in our films is determined from the XPS peak to be 2.00 ± 0.06. The O 1s signal reveals the presence of one large peak. The peak is located at binding energy of 531.2 eV, which is similar to the O 1s binding energy found for TiO_2. The shoulder is due to a small peak at 533 eV, which corresponds to SiO_2 present at the interface between silicon substrate and TiO_2 layer.

Figure 3 represents the core level spectra Si 2p and O 1s of the as deposited 3 nm SiO_2 film at room temperature using RF-sputtering. The observed binding energies are 99.4 eV for Si $2p_{3/2}$, 100 eV for Si $2p_{1/2}$, 103 eV for its oxide and 532.3 eV for O 1s. The atomic ratio O/Si of the SiO_2 prepared at room temperature is 2.00 ± 0.04. In our case, the separation of the Si 2p and SiO_2 is 3.63 eV (Leprince-Wang, 2002); (Wu et al, 1996).

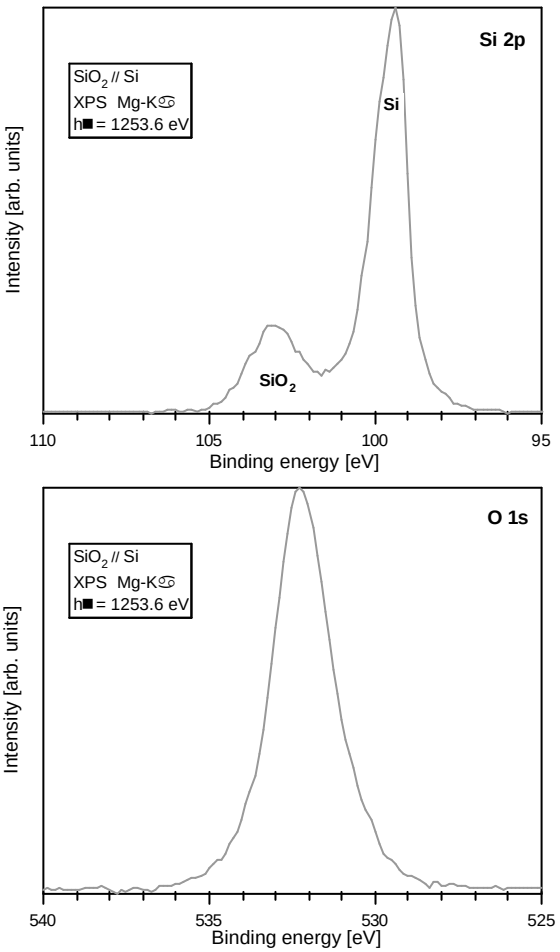

Fig. 3. XPS Si 2p and O 1s core-level spectra of the SiO_2

3.2 Laser Reflectometry

Real-time laser reflectometry is performed simultaneously to the dielectric layers deposited on silicon. Figure 4 shows the acquired reflectivity data during the deposition of stoichiometric TiO_2 and SiO_2. The polarisation of the laser light was parallel to the plane of the reflection (*p* polarized).

The resulting curves exhibit an oscillating behavior (two maxima and one minima for TiO_2; two maxima and two minima for SiO_2). For transparent films the amplitude of the oscillations is normally not attenuating during the deposition. These figures can be interpreted in a qualitative way. As the two maximum show the same value of reflectivity, the extinction coefficient *k* is zero as expected. We can directly deduce that the deposited films are transparent for both films TiO_2 and SiO_2. A quantitative determination of the optical constants is done by a numerical fit to the experimental data by using the formula for the reflectivity in the case of one layer on a substrate. The fit is represented as dashed line in figure 4.

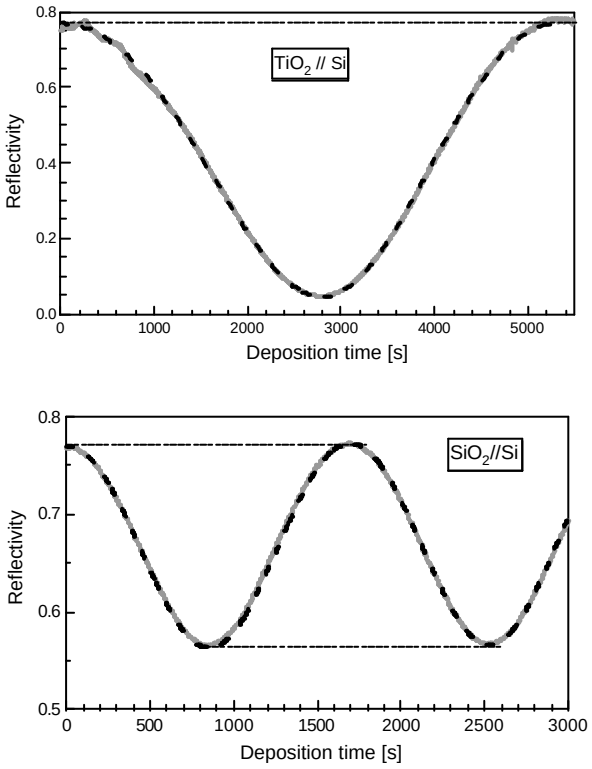

Fig. 4. Real-time laser reflectometry of sputtered TiO_2 and SiO_2 on Si. The solid curve corresponds to the experimental data, the dashed one to the fit curves and the dashed line indicates the position of the extrema.

In a straightforward way, laser reflectometry provides some important information such as growth rate, layer thickness and refractive *n* and extinction index *k* at one wavelength (532 nm) as represented in table 1 for TiO_2 and SiO_2 on silicon.

dielectric materials	***n***	***k***	V_d **[nm/min]**
TiO_2	2.2	0	1.0
SiO_2	1.47	0	7.6

Table. 1 *n*, *k* and V_d (deposition rate) of the sputtered stoichiometric TiO_2 and SiO_2 at λ = 532 nm

3.3 Ellipsometry

The ellipsometric data consist of the *y* and *D* spectra in the range 350 to 800 nm for different incident angles between 40° and 70°. As the optical ellipsometric characterization of an individual layer strongly depends on the choice of the appropriate model, the modelling of multilayer thin films becomes a complex task. The standard approach using reference data in the literature for the dielectric functions to determine the optical properties cannot be applied. Consequently, we have made a systematic study of the optical properties of individual dielectric layers, then of the more complex system of two layers and three layers. In this study, at first the model consists of a single film on silicon substrate. These data were fitted with a widely used Cauchy dispersion formula for both TiO_2 and SiO_2, where the refractive index *n* and extinction coefficients *k* are given by:

$$n(l) = n_0 + C_0 \frac{n_1}{l^2} + C_1 \frac{n_2}{l^4} \quad (2)$$

$$k(l) = k_0 + C_0 \frac{k_1}{l^2} + C_1 \frac{k_2}{l^4} \quad (3)$$

n_i, k_i, C_i are constants and l is the wavelength in nm. $C_0 = 10^2$ and $C_1 = 10^7$ are used to avoid large values of n_1, k_1, n_2 and k_2.

3.3.1. Individual layers on silicon substrates: TiO_2 // Si and SiO_2 // Si

Figure 5 and 6 show the measured *y* and *D* for deposited TiO_2 and SiO_2 on silicon substrate combined with the best theoretical fits using the Cauchy dispersion model. These films were modelled as a homogeneous dielectric layer on a semi-infinite silicon substrate. The native silicon oxide interlayer was included in the model. Surface roughness was neglected. Silicon and silicon oxide optical functions were taken from the literature (Palik,1985). The ambient refractive index is $n = 1$.

For a better visibility, the measurements and fits were plotted by solid and dashed lines respectively. A good agreement between the fit and the experimental data is observed, except below 350 nm.

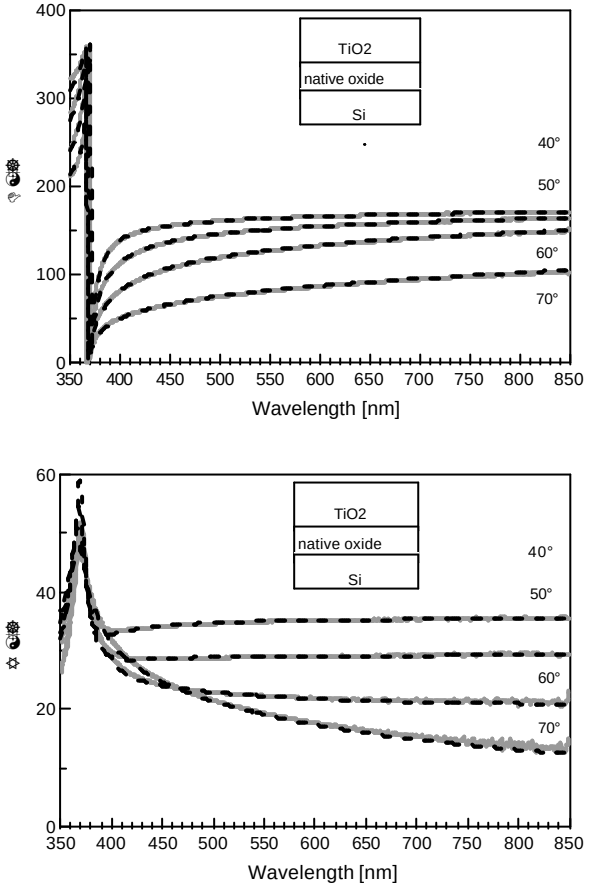

Fig. 5. Measured ellipsometric spectra of sputtered TiO_2 on silicon compared with the fit using a Cauchy model.

The best-fit parameters in the wavelength range 350 - 850 nm are given on table 2.

Parameter fit	TiO_2	SiO_2
n_0	2.38	1.46
n_1 [nm^2]	-899	25.3
n_2 [nm^4]	1781	17.5
k_0, k_1 [nm^2], k_2 [nm^4]	0	0

Table 2 Cauchy parameters for the sputtered TiO_2 and SiO_2 ellipsometry fits.

The results of the fit parameters confirm that no absorption occurs in the films. It should be noted here that the thickness of both TiO_2 and SiO_2 are in a good agreement and are within 5% of the determined one by the laser reflectometry.

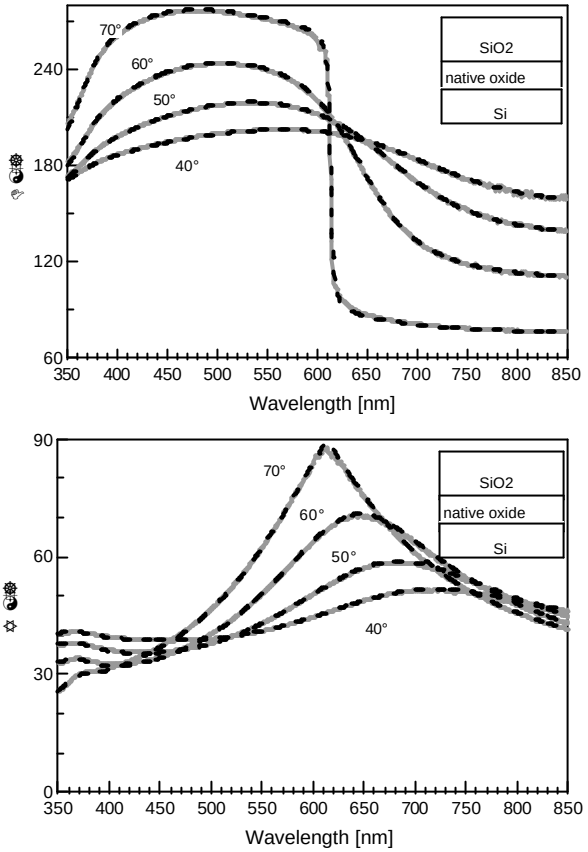

Fig. 6. Measured ellipsometric spectra of sputtered SiO_2 on silicon compared with the fit using a Cauchy model.

Figure 7 and 8 show the n and k as a function of the wavelength in the UV-Vis for TiO_2 and SiO_2 on silicon substrate as the result of the ellipsometric measurements and the fits.

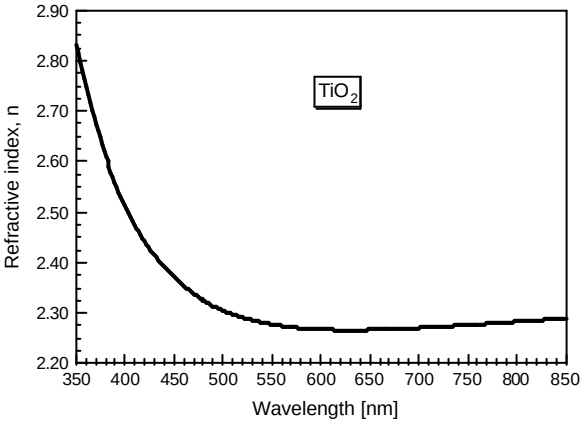

Fig. 7. Refractive index dispersion of TiO_2 in the UV-Vis range.

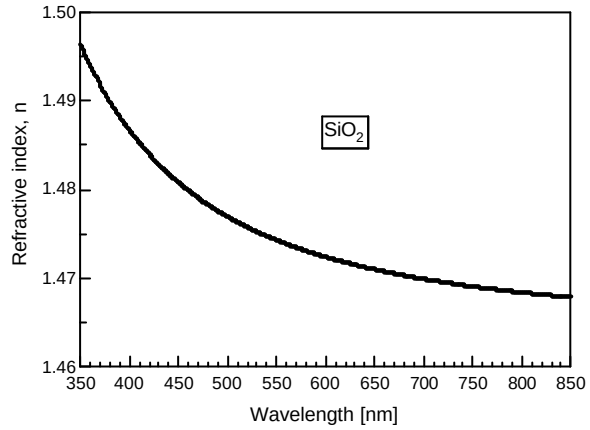

Fig. 8. Refractive index dispersion of SiO_2 in the UV-Vis range.

3.3.2 Triple layers on silicon substrates : TiO_2 // SiO_2 // TiO_2 // Si

We have deposited multilayer structures in order to test the validity of our model to fit the ellipsometric parameters. Figure 9 shows the measured *y* and *D* for TiO_2 on SiO_2 on TiO_2 on silicon substrate with the theoretical fit by Cauchy model from figures 7 and 8.

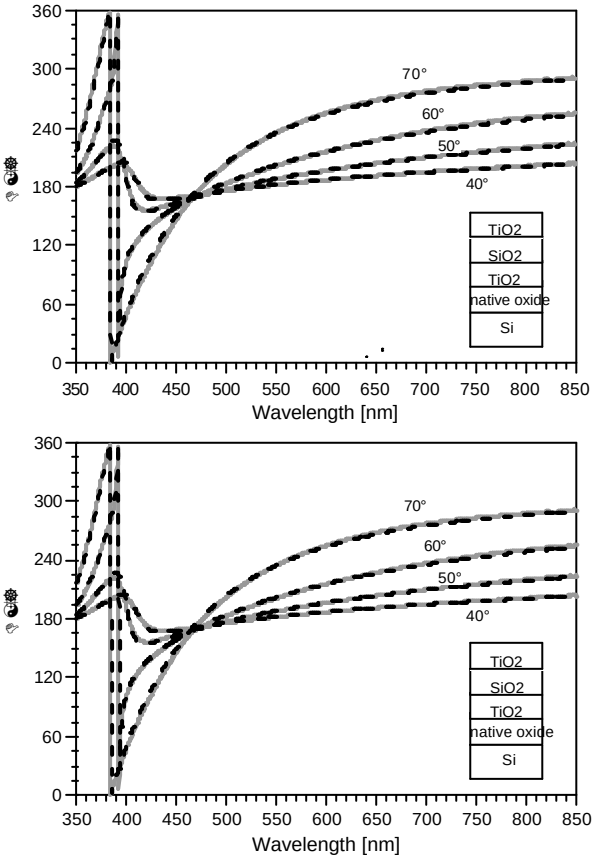

Fig. 9. Measured ellipsometric spectra of sputtered $TiO_2/SiO_2/TiO_2$ on silicon compared with the fit using a Cauchy model.

The optical constants values for the individual TiO_2 and SiO_2 layers obtained from the individual measurements of these materials (Figures 7 and 8) have been used for the the fit of multilayers.

The fair agreement between expected layer thickness determined from the deposition velocity by laser reflectometry and ellipsometry for individual layers and the measured thickness for the multilayer by ellipsometry indicate reproducible sputter deposition, the validity of our model and an abrupt interface between SiO_2 and TiO_2. This result confirms the reproducibility of the optical properties using our controlled sputtering deposition conditions and the applicability of our monolayer fit for more complex multilayer samples.

3.4 Transmission and reflectiviy

The total hemispherical reflectivity $R(l)$ and transmission $T(l)$ for the two single-layer samples TiO_2//glass and SiO_2//glass show a quasi-zero absorption of the films, confirming the results from laser reflectomerty and ellipsometry.

The multilayer sample is characterized by its solar transmis sion T_{sol} :

$$T_{sol} = \frac{\int T(l)\, I_{sol}(l)\, dl}{\int I_{sol}(l)\, dl} \tag{4}$$

We note here I_{sol} the intensity of the solar spectrum AM1.5.

To describe the colour of our multilayer film, we have chosen to use the three-dimensional *Lab* space 1976 (CIE Lab system). All existing colour can be represented using the coordinates *L*, *a* and *b*. The 1931 CIE Colour Matching Functions $x(l)$, $y(l)$ and $z(l)$ are used to calculate the normalized values X_x, Y_y, Z_z by integration the spectral distribution :

$$X_x = \frac{100}{95.047} \frac{\int R(l)\, D_{65}(l)\, x(l)\, dl}{\int D_{65}(l)\, y(l)\, dl} \tag{5}$$

$$Y_y = \frac{\int R(l)\, D_{65}(l)\, y(l)\, dl}{\int D_{65}(l)\, y(l)\, dl} \tag{6}$$

$$Z_z = \frac{100}{108.883} \frac{\int R(l)\, D_{65}(l)\, z(l)\, dl}{\int D_{65}(l)\, y(l)\, dl} \tag{7}$$

$D_{65}(l)$ is the standard illuminant. We then define the quantities X_v :

$$\begin{cases} \text{if } X_x > 0.008856: \ X_v = \sqrt[3]{X_x} & (8) \\ \text{if } X_x \le 0.008856: \ X_v = 7{,}787 \ X_x + \dfrac{16}{116} & (9) \end{cases}$$

The quantities Y_v and Z_v are defined similarly using Y_y and Z_z respectively. We finally have:

$$L = 116\ Y_v - 16 \quad (10)$$

$$a = 500\ (X_v - Y_v) \quad (11)$$

$$b = 200\ (Y_v - Z_v) \quad (12)$$

L, *a*, *b* form a three-dimensional coordinate system with *a* the red/green axis, *b* the yellow/blue axis and *L* the perpendicular luminosity axis.

Figure 10 shows the reflectivity for different multilayered samples. The calculated colour coordinates and the solar transmission are summarised in table 3.

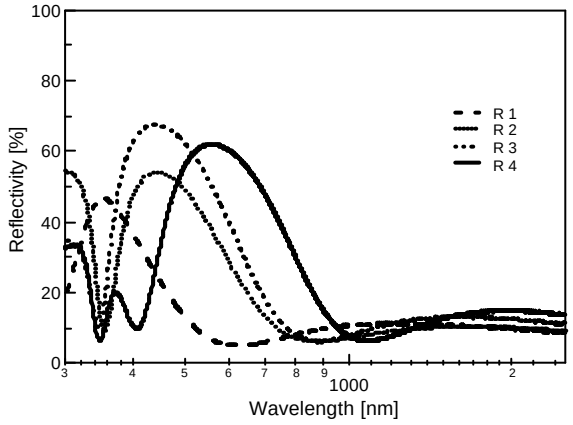

Fig. 10. Measured reflectivity of different multilayers on glass samples.

	T_{sol} [%]	a	b	colour of the reflected ligth
R 1	87.7	10.3	-34.9	blue
R 2	78.2	-10.5	-14.9	blue
R 3	72	-10.2	-15.57	blue-green
R 4	67.2	-11.9	26.5	green-yellow

Table 3. Solar transmission and calculated CIE Lab colour coordinates of different multilayers (presented in figure 10) on glass samples.

Different reflectivity peaks (up to 70 %) in the visible spectrum are observed by depositing on either two (R 1) or three (R 2, R 3, R 4) layers of TiO_2 and SiO_2 on glass substrate (figure 10). A solar transmission in the range 67% to 87% is obtained. A blue, blue-green and green-yellow colours are obtained by using double layered system and triple layered system as presented in table 3. For the double layered film the solar transmission is 87 % but for triple layered system is lower than 70%. However, the luminosity for triple layers is better. The result shows that the prepared coatings can meet the requirements for obtaining different reflected colours. More efforts are needed to improve at the same time the solar transmission and the luminosity.

4. CONCLUSION

In this work, coloured glass to cover solar collectors has been obtained by alternative deposition of dielectric layers with high and low refractive indices. The deposition rate has been controlled by in-situ laser reflectometry and confirmed by ex-situ ellipsometry for simple systems with one and three coating layers. The optical properties of the titanium oxide and silicon oxide have been determined. A Cauchy dispersion model is adequate for extracting the refractive and extinction index in the case of sputtering deposition.

The colour coordinates using the three-dimensional *Labs* space, blue, blue-green and green-yellow colours were calculated for two and three layers system. The reflected colour and the solar transmission depend on the thickness and the number of the alternative dielectric layers.

In conclusion, we have succeeded at first attempt to show that a sputtered multilayer coating can fulfilled the requirements:

- quasi-zero absorption
- coloured reflectivity peak in the visible
- acceptable solar transmission

More effort will be directed to optimize the thickness of individual layers and the number of layers for thermal solar collectors in order to get a higher solar transmission results, a reflected light accommodated in a narrower band and an appropriate colour for architectural integration in building.

ACKNOWLEDGEMENT

The authors wish to thank Roland Steiner for the technical support and Marc Ley for helpful discussions. This work is supported by the Swiss Federal Office of Energy and the Swiss National Science Foundation.

REFERENCES

Bhattacharyya D., Sahoo N.K., Thakur S., Das N.C. (2001), Vacuum, V. 60, pp. 419

Garapon C., Mugnier J., Panczer G., Jacquier B., Champeaux C., Marchet P. and Catherinot A. (1996), Appl. Surf. Science, V. 96-98, pp. 836

Ouellette M.F., Lang R.V., Yan K.L. Bertram R.W., Owies R.S. and Vincent D., (1991), J. Vac. Sci. Technol., A. 9, pp. 1188

Gomeza M.M., Beermannb N., Lua J., Olssona E., Hagfeldtb A., Niklassonb G.A., Granqvista C.G., (2003) Solar Energy Materials & Solar Cells, V. 76, pp. 37–56

Selhofer H. and Müller R. (1999), Thin Solid Films, V. 351, pp. 180

Zhong DishengXu Guangzhong and Liu Wi (1991), Vacuum, V. 42, N.16, pp. 1087

Martinet C., Paillard V., Gagnaire A. and Joseph J. (1997), Journal of Non-Crystalline Solids, pp. 77

Köstlin H., Frank G., Auding H. and Hebbinghaus G. (1997), Journal of Non-Crystalline Solids, V. 218, pp. 347

Que W., Sun Z., Zhou Y., Lam Y.L., Chan Y.C. and Kam C.H. (2000), Thin Solid Films, V. 359, Issue 2, pp. 177

Hill R.J. (1997), Journal of Non-Crystalline Solids V. 218, pp. 54

Vergöhl M., Malkomes N., Staedler T., Matthée T. and Richter U. (1999), Thin Solid Films, V. 351, Issue 1-2, pp. 42

Mardare D. and Rusu G.I. (2002), Materials Letters, V. 56, pp. 210

Gluck N.S., Sankur H., Heuer J., DeNatale J. and Gunning W.J. (1999), J. Appl. Phys, V.69, N.5, pp.3037

Tabata A., Matsuno N., Suzuoki Y. and Mizutani T (1996), Thin Solid Films, V. 289, pp. 84-89

Wong W., Masumoto H., Someno Y., Chen L. and Hirai T., (2000), J. Vac. Sci. Technol., A., V. 18, N. 3, pp. 933

Shirley D.A. (1972), Phys. Rev. B., V. 5, N. 1, pp. 4709

Yeh J.J. and Lindau I. (1985), Atomic Data and Nuclear Data Tables, V. 32, N. 1, pp. 2

Hesse R. (2002), www.uni-leipzig.de/unifit/

Heavens O.S. (1991), Optical properties of thin solid films

Schüler A., Ellenberger C., Oelhafen P., Haug C and Brenn R. (2000), J. Appl. Phys., V. 87, pp. 4285

Leprince-Wang Y. (2002), surface and coating technology, V. 150, pp. 257

Wu W.F. and Chiou B.S. (1996), Semicond. Sci. Technol., V. 11, pp. 1317

Palik E.D. (1985), Handbook of Optical Constants of Solids